JPET Fast Forward. Published on March 1, 2006 as DOI: 10.1124/jpet.106.101949

JPET #101949

Title Page

Potent Anti-Tumor Activity of a Novel Cationic Pyridinium-Ceramide Alone or In Combination with Gemcitabine Against Human Head and Neck Squamous Cell Carcinomas *In vitro* and *In vivo*

Can E. Senkal, Suriyan Ponnusamy, Michael J. Rossi, Kamala Sundararaj, Zdzislaw Szulc, Jacek Bielawski, Alicja Bielawska, Mario Meyer, Bengu Cobanoglu, Serap Koybasi, Debajyoti Sinha, Terry A. Day, Lina M. Obeid, Yusuf A. Hannun, and Besim Ogretmen

Departments of Biochemistry and Molecular Biology (C.E.S., S.P., Z.S., J.B., A.B., B.C., L.M.O., Y.A.H., B.O.), Hollings Cancer Center (A.B., M.M., T.A.D., L.M.O., Y.A.H., B.O.), Otolaryngology and Head and Neck Surgery (M.J.R., S.K., T.A.D.), Biostatistics, Bioinformatics and Epidemiology (D.S.), Medicine and Ralph H. Johnson Veterans Administration Hospital (L.M.O.), Medical University of South Carolina, Charleston, SC, USA.

JPET #101949

Running Title Page

Pyr-ceramide/gemcitabine inhibits HNSCC tumor growth

Corresponding author**:** Dr. Besim Ogretmen, Medical University of South Carolina, Department of Biochemistry, 173 Ashley Ave., Charleston, SC, 29424, USA. Tel: (843) 792 09 40 Fax: (843) 792 85 68 E-mail: ogretmen@musc.edu

Number of text pages: 38

Number of tables: 2

Number of figures: 7

Number of references: 39

Number of words in Abstract: 231

Number of words in Introduction: 814

Number of words in Discussion: 1155

Abbreviations: L-t-C_6-Pyr-Cer, L-threo-C_6-Pyridinium-Ceramide-bromide; HNSCC, human head and neck squamous cell carcinoma; UM-SCC-22A ,human SCC of the hypopharynx; LC/MS, liquid chromatography/mass spectroscopy; MTD, maximum tolerated dose; TRF Telomere Restriction Fragment; hTERT, human telomerase reverse transcriptase; SM, sphingomyelin; H&E, hematoxylin and eosin.

Abstract

In this study, a cationic water-soluble ceramide analogue L-threo-C_6-Pyridinium-Ceramide-bromide (L-t-C_6-Pyr-Cer), which exhibits high solubility and bio-availability, inhibited the growth of various human head and neck squamous cell carcinoma (HNSCC) cell lines at low IC_{50} concentrations, independent of their p53 status. Consistent with its design to target negatively charged intracellular compartments, L-t-C_6-Pyr-Cer accumulated mainly in mitochondria-, and nuclei-enriched fractions upon treatment of UM-SCC-22A cells (human SCC of the hypopharynx) at 1-6 hr. In addition to its growth inhibitory function as a single agent, the supra-additive interaction of L-t-C_6-Pyr-Cer with gemcitabine (GMZ), a chemotherapeutic agent used in HNSCC, was determined using isobologram studies. Then, the effects of this ceramide, alone or in combination with GMZ, on the growth of UM-SCC-22A xenografts in SCID mice was assessed following the determination of pre-clinical parameters, such as maximum tolerated dose (MTD), clearance from the blood, and bio-accumulation. Results demonstrated that treatment with L-t-C_6-Pyr-Cer in combination with GMZ significantly prevented the growth of HNSCC tumors *in vivo*. The therapeutic efficacy of L-t-C_6-Pyr-Cer/GMZ combination against HNSCC tumors was about 2.5-fold better than that of the combination of 5-fluorouracil (5-FU)/cisplatin (CP). In addition, LC/MS analysis showed that the levels of L-t-C_6-Pyr-Cer in HNSCC tumors were significantly higher than its levels in the liver and intestines, and interestingly, the combination with GMZ increased the sustained accumulation of this ceramide by about 40%. Moreover, treatment with L-t-C_6-Pyr-Cer/GMZ combination resulted in a significant inhibition of telomerase activity, and decrease in telomere length *in vivo*, which are among down-stream targets of ceramide.

Introduction

Human head and neck squamous cell carcinomas (HNSCC) are among five most common cancers in the world. Global occurrence of HNSCC is high, and it is estimated that about 780,000 new patients are diagnosed with HNSCC each year in the adult population. There are about 41,000 new HNSCC cases diagnosed annually in the United States in 2004, and the overall 5-year survival of patients with stage III and IV disease remains less than 50% (Her, 2001; Jemal et al. 2004).

Historically, chemotherapy did not play a curative role in the treatment of HNSCC, but was reserved for palliative therapy. Surgery and radiation therapy remained the primary curative options, however, complications of these therapies resulted in significant morbidity, cosmetic deformity, along with inability to speak, swallow, or chew. There is now increasing evidence that treatment combinations including chemotherapy offer improved cure rates when compared to standard therapies. Conventional chemotherapy of HNSCC in the clinic involves mainly the combination of cisplatinum (CP) with 5-fluorouracil (5-FU) or taxol (Cohen et al. 2004; Argiris et al. 2004). Recent studies have evaluated the combination of gemcitabine with a variety of anti-cancer agents such as vinorelbine, imatinib or cisplatinum with limited pharmacokinetic or synergistic interaction (Airoldi et al. 2003; Bruce et al. 2005; Jiang et al. 2005). Radiosensitization property of GMZ was also examined in patients with advanced HNSCC, and the data showed that the concurrent use of radiotherapy and gemcitabine was effective, but caused severe mucositis in the majority of patients (Aguilar-Ponce et al. 2004). Combination therapy involving anthracyclines against

these cancers has also been analyzed previously, with strict adherence to the dose limitations of these cardiotoxic compounds (Harrington et al. 2002). Despite these new treatment options, however, survival statistics for HNSCC have not improved significantly in decades (Her, 2001; Jemal et al. 2004). Therefore, the development of novel strategies is needed for the treatment of HNSCC.

The bioactive sphingolipid ceramide, an emerging tumor suppressor lipid, is known to regulate anti-proliferative responses, such as apoptosis, growth arrest, differentiation, and senescence in various human cancer cells (Ogretmen and Hannun, 2004). Many important biological targets and signaling events regulated by ceramide have been identified (Ogretmen and Hannun, 2004). Among these, telomerase activity has been detected in the majority of HNSCC tumors, and not in normal adjacent tissues (Fabricius et al. 2002; Koscielny et al. 2004). Moreover, increased telomerase activity in the tumors of HNSCC patients has been associated with high cell proliferation rates, and advanced pathologic stage (Patel et al. 2002), demonstrating that telomerase activity is one of the most important prognostic factors in HNSCC patients, and that telomerase can be an important target to develop novel therapeutic strategies for the treatment of these cancers (Tao et al. 2005).

Because of its anti-proliferative roles, exogenous ceramide has been used for the treatment of various human cancer cells both *in vitro* and *in vivo*. However, this approach presents some major challenges due to its: (i) very low water solubility and moderate/low cellular uptake, (ii) intracellular metabolism to complex sphingolipids, and (iii) uncontrolled

delivery, release and intracellular targeting. In order to overcome these problems, many biophysical and chemical approaches have been developed with improved delivery and bio-availability (Stover and Kester, 2003; Shabbits and Mayer, 2003). Another alternative approach has been the development of novel pyridinium ceramide analogs with increased water solubility, cell-membrane permeability, and cellular uptake as compared to their uncharged conventional ceramides (Rossi et al. 2005; Novgorodov et al. 2005). Pyridinium ceramides are designed to preferentially localize into negatively charged intracellular compartments, specifically mitochondria and nucleus, due to the presence of a positive charge delocalized over the π-electron system. The accumulation of D-erythro-C_6-Pyr-Cer specifically in mitochondria has been confirmed recently, and the data showed that mitochondrial localization of Pyr-Cer caused a decrease in its membrane potential, leading to cytochrome C release, and apoptosis (Novgorodov et al. 2005). In another independent study, anti-proliferative responses of L-t-C_6-Pyr-Cer, such as inhibition of cell cycle and telomerase activity, in HNSCC cell lines, but not in non-cancerous human adult keratinocytes and Wi-38 lung fibroblasts, were demonstrated (Rossi et al. 2005). The improved effects of L-t-C_6-Pyr-Cer in combination with gemcitabine (GMZ) in the inhibition of cell growth were also shown in HNSCC cells *in vitro* (Rossi et al. 2005). However, quantitative supra-additive interaction of these two compounds *in vitro*, or their therapeutic efficacy in the inhibition of HNSCC tumor growth *in vivo* has not yet been described.

In the present study, the data demonstrate that L-t-C_6-Pyr-Cer accumulates in mitochondria- and nuclei-enriched fractions in UM-SCC22A cells, which is consistent with its design

to target negatively charged sub-cellular compartments. In addition, it is shown here that L-t-C_6-Pyr-Cer inhibits the growth of various HNSCC cell lines at low IC_{50} concentrations, independent of their p53 status. Since single agents historically have not been very successful in the management and/or control of head and neck cancers in clinic, synergistic interaction between L-t-C_6-Pyr-Cer and GMZ in the inhibition of growth of HNSCC cells was shown by isobologram studies. More importantly, the *in vivo* therapeutic efficacy of L-t-C_6-Pyr-Cer in combination with GMZ, against HNSCC tumor growth was demonstrated using SCID mice harboring UM-SCC-22A xenografts. Moreover, it was shown here that the combination of L-t-C_6-Pyr-Cer with GMZ results in a significant modulation of telomerase activity, which appears to be regulated at the post-transcriptional level, concomitant with the reduced length of telomeres, *in vivo*.

Methods

Ceramides and chemotherapeutic agents. The novel water soluble cationic L-t-C_6-Pyr-Cer was synthesized by the Synthetic Lipidomics Core at the Department of Biochemistry and Molecular Biology, Medical University of South Carolina (MUSC) as described (Szulc Z. et al., unpublished data). Cetyl-pyridinium bromide (CPB) monohydrate was purchased from Aldrich. GMZ was obtained from Eli Lilly (Indianapolis, IN).

Cell lines and culture conditions. Human head and neck cancer cell lines UM-SCC-1 (retromolar trigone/floor of the mouth), UM-SCC-14A (SCC of anterior floor of the mouth), and UM-SCC-22A (SCC of hypopharynx) cells were obtained from Dr. Thomas Carey at the Department of Otolaryngology/Head and Neck Surgery, University of Michigan. Cells were grown in DMEM containing 10% FCS and 1% penicillin/streptomycin at 37^{o}C in 5% CO_2. Possible mycoplasma contaminations were monitored regularly by MycoAlert mycoplasma detection kit (Cambrex, ME), and treated with Plasmocin (InvivoGen; San Diego, CA), when/if necessary.

Subcellular fractionation, and the analysis of ceramide subspecies by mass spectroscopy (MS). The sub-cellular accumulation of L-t-C_6-Pyr-Cer was analyzed by utilizing normal phase high performance liquid chromatography and mass spectroscopy (LC/MS). The subcellular fractionations were done using differential centrifugation as described previously (Novgorodov et al. 2005). In short, cells were incubated in a buffer containing 300 mM sucrose, 10 mM Hepes (pH 7.4), 1 mM EDTA and 0.5 mM PMSF for 30 minutes on ice. The cells were then passed through 25-gauge needle for 5 strokes,

JPET Fast Forward. Published on March 1, 2006 as DOI: 10.1124/jpet.106.101949
This article has not been copyedited and formatted. The final version may differ from this version.

and centrifuged at 1,000× *g* for 10 min, 10,000× *g* for 10 min, and 100,000× g for 60 min at 4^{o}C, for collection of the nuclei-, mitochondria-enriched fractions, and microsomes, respectively. Each fraction was subjected to Western blotting with cytochrome C and lamin B antibodies to confirm the purity of mitochondrial and nuclear fractions.

MTT cell survival assay and isobologram studies. The concentrations of agents that inhibited cell growth by 50% (IC_{50}) were determined from cell survival plots obtained by MTT assays as described (Rossi et al., 2005). To determine the supra-additive interaction between L-t-C_6-Pyr-Cer and GMZ, isobologram plots (Steel and Peckham, 1979) were constructed using IC_{50} values of the two agents alone or in combination obtained from MTT assays. A straight line joining points on x- and y-axes represent the IC_{50} concentrations of GMZ and L-t-C_6-Pyr-Cer alone, and the points representing the IC_{50} concentrations of the combination of the two agents are represented as scatter plots on the same graphs. The points that fall within the left of the straight line indicate synergism. The experiments were performed as triplicates in at least 3 independent experiments. Error bars represent standard deviations.

Analysis of cell cycle profiles. The effects of L-t-C_6-Pyr-Cer, alone or in combination with GMZ, on the cell cycle profiles of UM-SCC-22A cells at various time points were analyzed in the presence of DNase-free RNase and propidium iodine (PI) by flow cytometry as described previously (Rossi et al., 2005). Untreated cells were used as controls.

JPET Fast Forward. Published on March 1, 2006 as DOI: 10.1124/jpet.106.101949
This article has not been copyedited and formatted. The final version may differ from this version.

Animal studies. The use of animals for determining the maximum tolerated dose (MTD), pharmacokinetics, and therapeutic efficacy of L-t-C_6-Pyr-Cer, alone or in combination with GMZ, were performed according to protocols which were approved by the Institutional Animal Care and Use Committee at the Medical University of South Carolina. The maximum tolerated dose (MTD) of L-t-C_6-Pyr-Cer was determined by dose escalation studies. In short, 7-week-old BALB/c mice (Taconic; Germantown, NY) were treated with increasing concentrations of the compound for various time intervals. Possible toxicity of the compound to the vital organs of the animals was analyzed by both gross examination, and histopathology. The accumulation of the compound in vital organs and in the serum was also determined by LC/MS as described previously (Koybasi et al., 2004). Blood counts, and enzyme assays were performed by Anilytics, Inc. (Gaithersburg, MD).

The role of L-t-C_6-Pyr-Cer, alone or in combination, in the inhibition of tumor growth *in vivo* was examined as follows: UM-SCC-22A cell xenografts were obtained by subcutaneous injection of 4 x 10^6 cells in the posterior flank of the female SCID mice (Taconic). After tumors were grown to at least 100 mm^3 (about two weeks after implantation), the mice were treated with various chemotherapeutic agents by intraperitoneal (IP) injection (alone or in combination) every 4 days for 24 days. Tumor volumes were calculated using the formula: length x $width^2$ x 0.52. Each experiment included 3 mice (which harbored two SCC tumors in their flanks) per each treatment, and experiments were done at least in two independent trials. The concentrations of the drugs used in this study were: L-t-C_6-Pyr-Cer (40 mg/kg), GMZ (40 mg/kg), DOX (1 mg/kg), 5-

FU (25 mg/kg), and CP (9 mg/kg). The known MTDs of these compounds are: 80, 120, 2, 25, and 9 mg/kg for L-t-C_6-Pyr-Cer (this study), GMZ, DOX, 5-FU and CP, respectively (Veerman et al., 1996; Inaba et al., 1989; Makino et al., 2001; van Moorsel et al., 1999).

Determination of telomerase activity, hTERT mRNA and protein levels in tumor tissues. Telomerase activity in tissues was measured by the PCR-based telomere repeat amplification protocol (TRAP) using TRAPeze kit (Invitrogen) which includes a 36-bp internal control to allow quantification of activity as described (Koybasi et al., 2004). The intensity of telomere-specific DNA bands, measured using Quantity One (BioRad) software, were normalized to the intensity of internal control bands for each sample on polyacrylamide gels for quantification. The mRNA levels of the catalytic subunit of telomerase, hTERT (human telomerase reverse transcriptase) was measured after extraction of total RNA from tumor tissues extracted from the control or treated animals, and normalized to mRNA levels of beta-actin by Applied Biosystems 7300 real-time quantitative PCR (Q-PCR) system using TaqMan primer and probe sets for hTERT and beta-actin (Applied Biosystems). The protein levels of hTERT in HNSCC tumors were determined by Western blot analysis using anti-hTERT rabbit polyclonal antibody (CalBiochem) at 1:1000 dilution. The specificity of the antibody was confirmed using extracts obtained from telomerase positive and negative cells by Western blotting.

Analysis of telomere length in tumor tissues. The measurement of telomere length was performed using total genomic DNA samples isolated from tumor tissues of the SCID mice using Telomere Restriction Fragment (TRF) Length measurement kit (Roche) by Southern

blotting as described previously (Sundararaj et al., 2004).

Statistical analysis. The statistical analysis of the animal studies to determine the therapeutic efficacy of the compounds in the inhibition of the growth of HNSCC tumors *in vivo* was performed using Tukey's Student Range Test and SAS-MIXED procedures.

Results

The sub-cellular localization of L-t-C_6-Pyr-Cer in UM-SCC-22A cells. Exogenous short chain ceramides are known to mediate cell cycle arrest, apoptosis or senescence in various cancer cells. However, because of their limited solubility and bio-availability, the water soluble pyridinium-conjugated analogues of ceramides were developed (Rossi et al., 2005; Novgorodov et al. 2005). Since previous data showed that D-e- and L-t-C_6-Pyr-Cer effectively inhibited the growth of UM-SCC-22A cells with a similar IC_{50} concentrations (Rossi et al., 2005), L-t-C_6-Pyr-Cer is used throughout this study because of its high solubility (Szulc, Z. M. et al. unpublished data). The chemical structure of L-t-C_6-Pyr-Cer is shown in Fig. 1A. Pyridinium ceramide (Pyr-Cer) analogues were designed to preferentially localize into negatively charged intracellular compartments, especially mitochondria and nucleus. Therefore, the sub-cellular accumulation of L-t-C_6-Pyr-Cer in UM-SCC-22A cells was examined using LC/MS after treatment with 1 μM L-t-C_6-Pyr-Cer for various time points (1, 3, 6, 12, 24 and 48 hr). The results showed that the compound mainly accumulated in the 10,000 x g fraction, which is enriched mainly in mitochondria, as early as 1 hr after treatment, and then it continued to increase to higher levels (1,000-3,000 pmol/0.1 mg protein) in this fraction between 3-48 hr treatment (Fig. 1B). Similarly, L-t-C_6-Pyr-Cer was detectable in the 1,000 x g fraction, which is enriched in nuclei, within 3 hr, and reached to 250-2,500 pmol/0.1 mg protein levels in this fraction between 6-48 hr (Fig. 1B). The amounts of the compound in the supernatant or the pellet of 100,000 x g fractions were either not detectable (at 1-6 hr), or minimal (at 12-48 hr) in these cells (Fig. 1B). The enrichment of mitochondria and nucleus in 10,000 x g and 1,000 x g fractions, respectively,

were confirmed by Western blotting with antibodies that detect the mitochondrial cytochrome C, and nuclear lamin B (Fig. 1C). Taken together, these data demonstrate that L-t-C_6-Pyr-Cer mainly accumulates in the mitochondria and, to a lesser extent, in the nucleus, within a short-time after exposure, as expected by its chemical composition and design.

The effects of L-t-C_6-Pyr-Cer, alone or in combination with GMZ, on the growth of HNSCC cells in vitro. To determine the effects of L-t-C_6-Pyr-Cer on growth, various HNSCC cell lines, which represent various forms of HNSCC were treated with increasing concentrations of L-t-C_6-Pyr-Cer for 48 hr, and its inhibitory concentration 50 (IC_{50}), a concentration that inhibits the growth by 50%, was determined by MTT assays as described in Materials and Methods. Consistent with our previous data (Rossi et al., 2005), L-t-C_6-Pyr-Cer inhibited the growth of human HNSCC cell lines UM-SCC-22A, UM-SCC-1, and UM-SCC14A cells with similar IC_{50} concentrations of about 1-2 μM at 48 hr (Fig. 1D). Since UM-SCC-1 cells express wild type p53, whereas UM-SCC-14A cells express mutated p53 (Bradford et al. 2003), their similar IC_{50} values for L-t-C_6-Pyr-Cer suggest that it may regulate cell growth independent of p53 status.

In the clinic, treatment of human HNSCC tumors with a single chemotherapeutic agent has not yielded much success, and therapies, which include the combination of two or more chemotherapeutic agents, such as 5-FU/CP or taxol/CP, appear to have more promising results (Argiris et al., 2004; Prevost et al. 2005). Therefore, we performed studies to test the growth inhibitory effects of L-t-C_6-Pyr-Cer in combination with various conventional

chemotherapeutic agents. Previous data (Rossi et al., 2005) showed that the combination of L-t-C_6-Pyr-Cer with gemcitabine (GMZ) improved its growth inhibitory effects against UM-SCC-22A cells, without any quantitative determination of supra-additivity (synergism). In this study, the supra-additive interaction between L-t-C_6-Pyr-Cer and GMZ in the inhibition of growth of UM-SCC-22A cells was evaluated using quantitative isobologram studies, as described in Materials and Methods. The data showed that the combination of L-t-C_6-Pyr-Cer at its sub-IC_{50} values (100, 250 and 500 nM) with increasing concentrations of GMZ for 48 hr decreased growth synergistically, as detected by the shift of the IC_{50} values of GMZ in the isobologram to the left of the line plot joining the x and y-axes that represent the IC_{50} of L-t-C_6-Pyr-Cer and GMZ, respectively (Fig. 2A). In addition, analysis of cell cycle profiles showed that treatment with L-t-C_6-Pyr-Cer in combination with GMZ (at 500 and 50 nM, respectively, for 48 hr) resulted in a cell cycle arrest at G0/G1, and decreased S-phase and G_2/M cell population as compared to controls (Fig. 2B). Interestingly, there was no apparent apoptosis in response to this combination treatment in these cells (Fig. 2B).

Determination of MTD, pharmacokinetics and bioaccumulation of L-t-C_6-Pyr-Cer in vivo. In order to evaluate the effects of L-t-C_6-Pyr-Cer in the inhibition of growth *in vivo*, its maximum tolerated dose (MTD) was determined by treatment of BALB/c mice with increasing concentrations of L-t-C_6-Pyr-Cer at 10-150 mg/kg for various time points. The data demonstrated that treatment of mice with a single dose of L-t-C_6-Pyr-Cer at 120-150 mg/ml resulted in toxicity resulting in extreme abdominal bloating and intestinal malfunction in some animals after about 6 hr of treatment (Table 1), whereas treatment with 10-80 mg/kg of the compound for 1-4 days did not have any detectable toxicity (Table 1).

Overall toxicity was determined by gross examination of the animals, and histo-pathological examination of the tissue sections obtained from brain, heart, lungs, liver, kidney, intestines, and bone marrow (data not shown). Thus, the MTD of L-t-C_6-Pyr-Cer was determined as 80 mg/kg in mice, which did not cause any detectable toxicity in these animals after either single (Table 1), or multiple cycles (every 4 days for 20 days) of treatment (data not shown).

Next, the pharmacokinetic parameters of L-t-C_6-Pyr-Cer, such as clearance from the blood, and bioaccumulation in various organs, were examined by LC/MS after treatment with the compound at 40 mg/ml (half of the MTD that would be used for the *in vivo* therapeutic studies) for various time points. As shown in Fig. 3A, the serum levels of the compound reached 4,500 to 6,500 pmol/0.1 ml serum at 0.5-2 hr, respectively, and cleared from the serum within 4 hr. The levels of the compound increased slightly first in the intestines after 5 min, and in the liver after 2 hr, which were about 600 and 500 pmol/mg protein, respectively (Fig. 3B). The compound started to accumulate mainly in the kidney between 4-8hr (Fig. 3B). There was some accumulation in the lungs after 24 hr, and no significant accumulation in the brain or heart (Fig. 3B). These data suggest that L-t-C_6-Pyr-Cer circulates through systemic delivery within 2-4 hr, and accumulates in the intestines, liver and lungs at moderate levels, and at high levels in the kidneys within 8-24 hr, possibly for excretion. These data are consistent with previous studies, which showed the main accumulation of other lipophilic pyridinium cations in the kidneys, and excretion in the urine (Pietruck et al. 1995).

JPET Fast Forward. Published on March 1, 2006 as DOI: 10.1124/jpet.106.101949
This article has not been copyedited and formatted. The final version may differ from this version.

The inhibition of HNSCC tumor growth by L-t-C_6-Pyr-Cer as compared to its conventional analogue L-t-C_6-Cer in vivo. After determining the MTD, pharmacokinetic and bioaccumulation parameters, the therapeutic efficacy of L-t-C_6-Pyr-Cer against HNSCC xenografts, which were developed by subcutaneous injection of UM-SCC-22A cells to both sides of the flank of the SCID mice, was assessed, and compared to the effects of L-t-C_6-Cer (without the pyridinium moiety) as described in Experimental Procedures. After the tumors were established (at least 100 mm^3 in volume), mice were treated with 40 mg/kg ceramides every 4 days for 6 cycles (total of 24 days). The histo-pathological analysis of the tumors confirmed that they were SCC (Fig. 4A). More importantly, as shown in Fig. 4B, the growth of HNSCC tumors was significantly inhibited by L-t-C_6-Pyr-Cer when compared to untreated controls ($p<0.001$). In addition, these data also showed that the tumor inhibitory effects of L-t-C_6-Pyr-Cer were about 2.5-fold greater than conventional L-t-C_6-Cer (Fig. 4B).

The therapeutic efficacy of L-t-C_6-Pyr-Cer in combination with GMZ in the inhibition of HNSCC tumor growth *in vivo.* Next, the therapeutic efficacy of L-t-C_6-Pyr-Cer in combination with GMZ against HNSCC tumors was examined in vivo. After the tumors were established (the average initial tumor volumes were 165, 286, 413, 120 and 268 mm^3 for control, GMZ, L-t-C_6-Pyr-Cer, 5-FU/CP and L-t-C_6-Pyr-Cer/GMZ, respectively), the animals were treated with L-t-C_6-Pyr-Cer or GMZ, alone or in combination at 40 mg/kg/each (at or below their half of MTDs), every 4 days for 24 days. As Fig. 5A shows, treatment with L-t-C_6-Pyr-Cer or GMZ as single agents caused some inhibition of HNSCC

tumor growth *in vivo* as compared to untreated controls. However, the combination of L-t-C_6-Pyr-Cer with GMZ almost completely inhibited the tumor growth ($p < 0.01$), and the efficacy of this combination was about 2.5-fold better than that of 5-FU/CP ($p<0.05$) (Fig. 5A). Importantly, treatment of animals with L-t-C_6-Pyr-Cer alone or in combination with GMZ did not cause any significant changes (not more than 5%) in the total body weight of the animals (data not shown). Treatment of SCID mice bearing UM-SCC-22A xenografts with 40 mg/kg cetylpyridinium bromide (without ceramide conjugate) for 4 days was lethal to all animals tested (n=6, data not shown). Also, combination of L-t-C_6-Pyr-Cer (40 mg/kg) with doxorubicin (1 mg/kg) was toxic to the animals (n=6), killing all the animals at day 2-3 of treatment (data not shown).

To confirm the lack of toxicity in response to L-t-C_6-Pyr-Cer/GMZ treatment, tumors and the vital organs were surgically removed after the completion of the study, and hematoxylin and eosin (H&E) staining of the tissue sections was performed as described. Analysis of the vital organs of the animals treated with L-t-C_6-Pyr-Cer alone or in combination with GMZ showed no detectable toxicity (data not shown). Blood counts, levels of enzyme activities, and electrolytes in the serum of animals (such as red blood cell and hemoglobin, blood urea nitrogen, creatinine, Na, Mg, alanine amino transferase and amylase) after these treatments were also analyzed (Table 2). There were no detectable abnormalities in these levels, confirming the lack of overall toxicity.

Interestingly, analysis of the levels of L-t-C_6-Pyr-Cer in HNSCC tumors removed after the completion of the study by LC/MS, showed that its accumulation in the tumor site was

about 2,200 pmol/mg when used as a single agent, whereas its levels in the tumors increased about 40% (up to 3,100 pmol/mg) when combined with GMZ (Fig. 5B). The levels of the compound in the intestines and the liver in the absence of GMZ were about 120 and 100 pmol/mg protein, which increased to 1,000 and 300 pmol/mg protein in the presence of GMZ. Thus, these data demonstrate that the levels of the compound in tumors were about 3-6-fold higher than its levels in intestines or liver of the animals, in the absence or presence of GMZ (Fig. 5B). Analysis of the effects of L-t-C_6-Pyr-Cer, alone or in combination of GMZ, on the endogenous levels of ceramide in tumor site (Fig. 6A and B), or in the vital organs (data not shown) of the animals showed that treatments with L-t-C_6-Pyr-Cer, alone or in combination with GMZ, did not cause any sustained elevation of endogenous ceramides when compared to untreated controls (Fig. 6A and B), suggesting that it does not affect the long-term metabolism of endogenous ceramide directly or indirectly. Similar data were also observed for the endogenous sphingomyelin (SM) levels, in which no significant changes were observed in response to these treatments when compared to untreated controls (data not shown).

Role of L-t-C_6-Pyr-Cer in combination with GMZ in the regulation of telomerase in vivo. To examine whether the inhibition of HNSCC tumor growth in response to L-t-C_6-Pyr-Cer, alone or in combination with GMZ, mechanistically involves the inhibition of telomerase *in vivo*, the levels of enzyme activity, hTERT mRNA and protein levels were measured in tumor extracts by TRAP, Q-PCR and Western blotting, respectively, as described in Materials and Methods. As shown in Fig. 7A, telomerase activity was inhibited significantly in HNSCC tumors of the animals treated with the combination of L-t-C_6-Pyr-

JPET Fast Forward. Published on March 1, 2006 as DOI: 10.1124/jpet.106.101949
This article has not been copyedited and formatted. The final version may differ from this version.

Cer and GMZ by about 60%, which was concomitant with a significant reduction of TRF length (about 700 bp) in these tumors as compared to untreated controls (Fig. 7B, lanes 5 and 2, respectively). Treatment with L-t-C_6-Pyr-Cer and GMZ as single agents also caused attrition in telomere length, about 500 and 200 bp, respectively, as compared to controls (Fig. 7B, lanes 4, 3 and 2, respectively).

Consistent with the proposed mechanisms of action of ceramide in the regulation of telomerase activity at the mRNA levels of hTERT in various human cancer cell lines *in vitro*, the inhibition of telomerase by L-t-C_6-Pyr-Cer (Fig. 7A) correlated with decreased levels of hTERT mRNA, and protein expression when compared to controls *in vivo* (Fig. 7C, and 7D, lanes 3 and 1, respectively). However, although treatment with the combination of L-t-C_6-Pyr-Cer and GMZ did not cause any detectable changes in the mRNA levels of hTERT (Fig. 7C), its protein levels were significantly inhibited (Fig. 7D, lane 4) in response to this combination, indicating a post-transcriptional regulation. The protein levels of beta-actin in these samples were used as loading controls (Fig. 7D, lower panel).

Taken together, these data demonstrate, for the first time, that treatment with the combination of L-t-C_6-Pyr-Cer with GMZ results in a significant inhibition of telomerase activity, and decreased telomere length in HNSCC tumors *in vivo*. Mechanistically, *in vivo* modulation of telomerase activity by this combination appears to be at the post-transcriptional level, resulting in a significant decrease on the levels of hTERT protein.

Discussion

In the present study, the growth inhibitory roles of L-t-C_6-Pyr-Cer, alone or in combination with GMZ, against HNSCC cells both *in vitro* and *in vivo* were examined. It was demonstrated here that L-t-C_6-Pyr-Cer accumulates mainly in the mitochondria- and nuclei-enriched sub-cellular fractions, which is consistent with its design and targeting. The data also showed that L-t-C_6-Pyr-Cer significantly inhibits the growth of various HNSCC cell lines at low IC_{50} concentrations, independent of their p53 status. This might be very important for its potential use against variety of cancers, since majority of cancer cells contain mutated p53 (Don and Hogg, 2004). The supra-additive effects of L-t-C_6-Pyr-Cer in combination with GMZ on the inhibition of HNSCC cell growth were also determined by quantitative isobologram studies, *in vitro*. More importantly, after preclinical parameters were determined, the data revealed that treatment with L-t-C_6-Pyr-Cer/GMZ in combination almost completely inhibited tumor growth in the xenograft models of HNSCC in SCID mice, which was much more effective than the effects of 5-FU/CP combination against these tumors. The LC/MS analysis showed that the levels of L-t-C_6-Pyr-Cer in the tumor site are significantly higher than its levels in the liver and intestines, and interestingly, the combination with GMZ increased the sustained accumulation of this ceramide. Moreover, the inhibition of HNSCC tumor growth and/or progression by L-t-C_6-Pyr-Cer/GMZ was concomitant with the inhibition of telomerase, and decrease in telomere length, which are among the cancer-specific nuclear down-stream targets of ceramide (Ogretmen and Hannun, 2004). The modulation of telomerase *in vivo* was regulated at the post-transcriptional level of hTERT protein, leading to a significant decrease in the levels of hTERT in response to

this combination.

Because of inherent limitations in the solubility and bioavailability of conventional exogenous ceramides, novel cationic ceramides with high water solubility, cell-membrane permeability and cellular uptake have been designed and synthesized (Rossi et al., 2005; Novgorodov et al., 2005). The presence of the positive charge in the pyridinium ring was designed to target and accumulate these ceramide analogues into negatively charged intracellular compartments, especially mitochondria and nucleus. Previous studies have also demonstrated that the majority of cancer cells acquire high levels of negative charge in their sub-cellular structures, such as in mitochondria and/or nuclei (Modica-Napolitano and Aprille, 2001), suggesting that pyridinium-ceramides may prefentially accumulate in cancer cells. Indeed, in this study, the accumulation of L-t-C_6-Pyr-Cer preferentially in mitochondria-, and nuclei-enriched fractions was established in UM-SCC-22A cells *in vitro*, and this was also consistent with the higher accumulation of the compound in the tumor site than in the liver and intestines *in vivo*. The accumulation of Pyr-Cer in mitochondria has been shown in HepG2 and MCF-7 cells previously, and this caused dramatic alterations in the structures and functions of mitochondria, resulting in apoptotic cell death (Novgorodov et al., 2005). However, effects of L-t-C_6-Pyr-Cer on the modulation of telomerase, and decrease in telomere length in HNSCC *in vivo* also suggest an important role for its nuclear accumulation. It should be noted also that, in addition to pyridinium-conjugated compounds, there are other compounds, such as F16 and jasmonates, which were shown to accumulate in mitochondria (Fantin and Leder, 2004, Rotem et al., 2005).

The role of exogenous ceramides in mediating anti-proliferative functions in various human

JPET Fast Forward. Published on March 1, 2006 as DOI: 10.1124/jpet.106.101949
This article has not been copyedited and formatted. The final version may differ from this version.

cancer cells has been demonstrated previously. For example, novel structural analogs of ceramide, such as C_{16}-serinol and (2S,3R)-(4E,6E)-2-octanoylamidooctadecadiene-1,3-diol (4,6-diene-ceramide) mediated apoptosis in neuroblastoma and breast cancer cells, respectively (Bieberich et al., 2000; Struckhoff et al. 2004). Other ceramide analogs, 5R-OH-3E-C8-ceramide, adamantyl-ceramide and benzene-C_4-ceramide displayed selective growth inhibitory roles in drug resistant human breast cancer cell lines (SKBr3 and MCF-7/Adr) (Crawford et al. 2003).

In an alternative approach, delivery of exogenous ceramide in cationic pegylated liposomes increased accumulation of ceramide, and enhanced its ability to kill breast cancer cells (Stover and Kester, 2003). The liposomal delivery of exogenous natural ceramide also resulted in the inhibition of phosphorylated Akt, and stimulated the activity of caspase-3/7 more effectively than non-liposomal ceramide (Stover and Kester, 2003). Recently, promising *in vivo* therapeutic efficacy of these pegylated liposomes used for the delivery of exogenous ceramide was shown in breast cancer models (Stover et al., 2005).

Clinical data suggest that head and neck cancers respond better to chemotherapy regimens, which include combinations of two or more anti-cancer agents (Kroep et al. 1999). Indeed, the conventional chemotherapy for these cancers is the combination of CP with 5-FU or taxol (Kroep et al. 1999). Therefore, in this study, the effects of treatment with L-t-C_6-Pyr-Cer in combination with GMZ in the inhibition of HNSCC tumor growth and/or progression was examined *in vivo*, and the data revealed the superior therapeutic efficacy of this combination over the conventional CP/5-FU treatment. The use of GMZ for the treatment of

HNSCC in combination with CP, imatinib or vinca alkoloids has been reported previously (Airoldi et al., 2003; Bruce et al., 2005; Kroep et al., 1999; Jiang et al., 2005). Also, GMZ was known to sensitize HNSCC cells to radiation (Aguilar-Ponce et al., 2004). However, these studies reported some toxicity, which limit their therapeutic significance. Since there was no detectable overall toxicity in animals treated with the combination of L-t-C_6-Pyr-Cer and GMZ, it would be interesting to test the efficacy of combining L-t-C_6-Pyr-Cer/GMZ with radiotherapy for the treatment of HNSCC in future studies. Interestingly, the data presented here showed that treatment with GMZ enhanced the accumulation of L-t-C_6-Pyr-Cer significantly in the HNSCC tumors *in vivo*, which might be very important for their improved efficacy against these tumors. The mechanisms by which GMZ increases in-tumor accumulation of this compound, however, are still unknown, and needs to be determined.

Moreover, the role of both endogenous and exogenous ceramides in the inhibition of telomerase function in various human cancer cells *in vitro* has been demonstrated previously (Ogretmen et al., 2001; Wooten and Ogretmen, 2005). Modulation of telomerase by ceramide has been mainly regulated at the transcriptional level of hTERT in human cancer cells in vitro (Wooten and Ogretmen, 2005). However, results presented here showed that treatment with the combination of L-t-C_6-Pyr-Cer/GMZ inhibited telomerase at the pos-transcriptional level *in vivo*. The mechanisms by which Pyr-Cer/GMZ combination treatment results in decreased levels of hTERT protein *in vivo*, however, are still unknown, and need to be determined. Interestingly, there are data, which implicate the involvement of ubiquitin/proteasome pathway for the regulation of hTERT in some cells (Kim et al., 2005). Also, role of ceramide in the regulation of c- Myc via increased ubiquitination, and

proteasome degradation has been shown previously in A549 human lung cancer cells (Ogretmen et al., 2001). Therefore, it would be important to examine whether decreased levels of hTERT protein in response to this combination is regulated by ubiquitin/proteasome pathway.

In summary, the results presented here suggest that treatment with water soluble L-t-C_6-Pyr-Cer in combination with GMZ inhibits HNSCC tumor growth and/or progression with no detectable overall toxicity *in vivo*, suggesting that the combination of these two compounds might provide alternative strategies for the improved management/control of HNSCC.

Acknowledgements

We thank Dr. P. Hall (School of Pharmacy, MUSC) for helping us design animal studies. We also are grateful to Dr. T. Carey (University of Michigan) for providing us with the HNSCC cell lines. Analysis of cell cycle profile was performed by the Hollings Cancer Center Flow Cytometry Core Facility at MUSC.

References

Aguilar-Ponce J, Granados-Garcia M, Villavicencio V, Poitevin-Chacon A, Green D, Duenas-Gonzalez A, Herrera-Gomez A, Luna-Ortiz K, Alvarado A, Martinez-Said H, Castillo-Henkel C, Segura-Pacheco B, De la Garza J (2004) Phase II trial of gemcitabine concurrent with radiation for locally advanced squamous cell carcinoma of the head and neck. *Ann Oncol* **15**:301-306.

Airoldi M, Cattel L, Cortesina G, Giordano C, Passera R, Pedani F, Novello S, Bumma C, Gabriele P (2003) Gemcitabine and vinorelbine in recurrent head and neck cancer: pharmacokinetics and clinical results. *Anticancer Res* **23**: 2845-2852.

Argiris A, Li Y, Murphy BA, Langer CJ, Forastiere AA (2004) Outcome of elderly patients with recurrent or metastatic head and neck cancer terated with cisplatin-based chemotherapy. *J Clin Oncol* **22**: 262-268.

Bieberich E, Kawaguchi T, Yu RK (2000) *N*-acylated serinol is a novel ceramide mimic inducing apoptosis in neuroblastoma cells. *J Biol Chem* **275**:177–181

Bradford CR, Zhu S, Ogawa H, Ogawa T, Ubell M, Narayan A, Johnson G, Wolf GT, Fisher SG, Carey TE (2003) P53 mutation correlates with cisplatin sensitivity in head and neck squamous cell carcinoma lines. *Head Neck* **25**:654-661.

Bruce IA, Slevin NJ, Homer JJ, McGown AT, Ward TH (2005) Synergistic effects of imatinib (STI 571) in combination with chemotherapeutic drugs in head and neck cancer. *Anticancer Drugs* **16**:719-726.

Cohen EE, Lingen MW, Vokes EE (2004) The expanding role of systemic therapy in head and neck cancer. *J Clin Oncol* **22**:1743-1752.

Crawford KW, Bittman R, Chun J, Byun HS, Bowen WD (2003) Novel ceramide analogs display selective cytotoxicity in drug-resistant breast tumor cell lines compared to normal breast epithelial cells. *Cell Mol Biol* **49**:1017–1023.

Don AS, Hogg PJ (2004) Mitochondria as cancer drug targets. *Trends Mol Med* **10**:372-378.

Fabricius EM, Gurr U, Wildner GP (2002) Telomerase activity levels in the surgical margin and tumour distant tissue of the squamous cell carcinoma of the head and neck. *Anal Cell Pathol* **24**: 25-39.

Fantin VR, Leder P (2004) F16, a mitochondriotoxic compound, triggers apoptosis or necrosis depending on the genetic background of the target carcinoma cell. *Cancer Res* **64**:329-336.

Harrington KJ, Lewanski C, Northcote AD, Whittaker J, Peters AM, Vile RG, Stewart JS (2001) Phase II study of pegylated liposomal doxorubicin (Caelyx) as induction chemotherapy for patients with squamous cell cancer of the head and neck. *Eur J Cancer* **37**: 2015-2022.

Her C (2001) Nasopharyngeal cancer and the Southeast Asian patient. Am Fam Physician **63**:1776-1782.

Inaba M, Kobayashi T, Tashiro T, Sakurai Y, Maruo K, Ohnishi Y, Ueyama Y, Nomura T (1989) Evaluation of antitumor activity in a human breast tumor/nude mouse model

with a special emphasis on treatment dose. *Cancer* **64**:1577-1582

Jemal A, Murray T, Ward E, Samuels A, Tiwari RC, Ghafoor A, Feuer EJ, Thun MJ (2004) Cancer Statistics 2004. *CA Cancer J Clin* **54**:8-29.

Jiang Y, Wei YQ, Luo F, Zou LQ, Liu JY, Peng F, Huang MJ, He QM (2005) Gemcitabine and cisplatin in advanced nasopharyngeal carcinoma: a pilot study. *Cancer Invest* **23**:123-128.

Kim JH, Park SM, Kang MR, Oh SY, Lee TH, Muller MT, Chung IK (2005) Ubiquitin ligase MKRN1 modulates telomere length homeostasis through a proteolysis of hTERT. *Genes Dev* **19**:776-781.

Koybasi S, Senkal CE, Sundararaj K, Spassieva S, Bielawski J, Osta W, Day TA, Jiang JC, Jazwinski SM, Hannun YA, Obeid LM, Ogretmen B (2004) Defects in cell growth regulation by C18:0-ceramide and longevity assurance gene 1 in human head and neck squamous cell carcinomas. *J Biol Chem* **279**:44311-44319.

Kroep JR, Peters GJ, van Moorsel CJ, Catik A, Vermorken JB, Pinedo HM, van Groeningen CJ (1999) Gemcitabine-cisplatin: a schedule finding study. *Ann Oncol* **10**:1503-1510.

Makino M, Shoji H, Takemoto D, Honboh T, Nakamura S, Kurayoshi K, Kaibara N (2001) Comparative study between daily and 5-days-a-week administration of 5-fluorouracil chemotherapy in mice: determining the superior regimen. *Cancer Chemother Pharmacol* **48**:370-374.

Modica-Napolitano JS, Aprille JR (2001). Delocalized lipophilic cations selectively target the mitochondria of carcinoma cells. *Adv Drug Deliv Rev* **49**:63-70.

Novgorodov SA, Szulc ZM, Luberto C, Jones JA, Bielawski J, Bielawska A, Hannun YA, Obeid LM (2005) Positively charged ceramide is a potent inducer of mitochondrial permeabilization. *J Biol Chem* **280**:16096-16105.

Ogretmen B, Kraveka JM, Schady D, Usta J, Hannun YA, Obeid LM (2001) Molecular mechanisms of ceramide-mediated telomerase inhibition in the A549 human lung adenocarcinoma cell line. *J Biol Chem* **276**:32506-32514.

Ogretmen B and Hannun YA (2004) Biologically active sphingolipids in cancer pathogenesis and treatment. *Nature Rev Cancer* **4**: 604–616.

Patel MM, Parekh LJ, Jha FP, Sainger RN, Patel JB, Patel DD, Shah PM, Patel PS (2002) Clinical usefulness of telomerase activation and telomere length in head and neck cancer. *Head Neck* **24**:1060-1067.

Pietruck F, Ullrich KJ (1995). Transport interactions of different organic cations during their excretion by the intact rat kidney. *Kidney Int* **47**:1647-1657.

Prevost A, Merol JC, Aime P, Moutel K, Roger-Liautaud F, Nasca S, Legros M, Coninx P (2005) A randomized trial between two neoadjuvant chemotherapy protocols: CDDP + 5-FU versus CDDP + VP16 in advanced cancer of the head and neck. *Oncol Rep* **14**:771-776.

Rossi MJ, Sundararaj K, Koybasi S, Phillips MS, Szulc ZM, Bielawska A, Day TA, Obeid LM, Hannun YA, Ogretmen B (2005) Inhibition of growth and telomerase activity by novel cationic ceramide analogs with high solubility in human head and neck squamous

cell carcinoma cells. *Otolaryngol Head Neck Surg* **132**:55-62.

Rotem R, Heyfets A, Fingrut O, Blickstein D, Shaklai M (2005) Jasmonates: Novel anticancer agents acting directly and selectively on human cancer cell mitochondria. *Cancer Res* **65:**1984-1993.

Shabbits JA, Mayer LD (2003) Intracellular delivery of ceramide lipids via liposomes enhances apoptosis in vitro. *Biochim Biophys Acta* **1612**:98-106.

Steel GG, Peckham MJ (1979) Exploitable mechanisms in combined radiotherapy-chemotherapy: The concept of additivity. *Int J Radiat Oncol Biol Phys* **5**:85-93.

Stover T, Kester M (2003) Liposomal delivery enhances short-chain ceramide-induced apoptosis of breast cancer cells. *J Pharmacol Exp Ther* **307**:468-475.

Stover TC, Sharma A, Robertson GP, Kester M (2005). Systemic delivery of liposomal short-chain ceramide limits solid tumor growth in murine models of breast adenocarcinoma. *Clin Cancer Res* **11**:3465-3474.

Struckhoff AP, Bittman R, Burow ME, Clejan S, Elliott S, Hammond T, Tang Y, Beckman BS (2004) Novel ceramide analogs as potential chemothrapeutic agents in breast cancer. *J Pharmacol Exp Ther* **309**:523–532.

Sundararaj KP, Wood RE, Ponnusamy S, Salas AM, Szulc Z, Bielawska A, Obeid LM, Hannun YA, Ogretmen B (2004) Rapid shortening of telomere length in response to ceramide involves the inhibition of telomere binding activity of nuclear glyceraldehyde-3-phosphate dehydrogenase. *J Biol Chem* **279**:6152-6162.

Tao Z, Chen S, Wu Z, Xiao B, Liu J, Hou W (2005). Targeted therapy of human laryngeal squamous cell carcinoma in vitro by antisense oligonucleotides directed against telomerase reverse transcriptase mRNA. *J Laryngol Otol* **119**:92-96.

van Moorsel CJ, Pinedo HM, Veerman G, Vermorken JB, Postmus PE, Peters, GJ (1999) Scheduling of gemcitabine and cisplatin in Lewis lung tumour bearing mice. *Eur J Cancer* **35**:808-814.

Veerman G, Ruiz van Haperen VW, Vermorken JB, Noordhuis P, Braakhuis BJ, Pinedo HM, Peters GJ (1996) Antitumor activity of prolonged as compared with bolus administration os 2',2'-difluorodeoxycytidine in vivo against murine colon tumors. *Cancer Chemother Pharmacol* **38**:335-342.

Wooten LG, Ogretmen B (2005) Sp1/Sp3-dependent regulation of human telomerase reverse transcriptase promoter activity by the bioactive sphingolipid ceramide. *J Biol Chem* **280**:28867-28876.

Footnotes

This work was supported by research grants from the National Institutes of Health CA88932, DE01657 (B.O.), CA097132 (Y.A.H.), and AG16583 (L.M.O.), Department of Defense, phase VII program project grant through Hollings Cancer Center (B.O.), and the National Science Foundation/EPSCoR, EPS-0132573 (B.O.). The animal facility used in this study was supported by the National Institutes of Health, Grant Number C06 RR015455 (MUSC) from the Extramural Research Facilities Program of the National Center for Research Resources.

Figure Legends

Fig. 1. The sub-cellular accumulation, and growth inhibitory properties of L-t-C_6-Pyr-Cer in HNSCC cells. A) Chemical structure of L-t-C_6-Pyr-Cer is shown. B) The subcellular accumulation of L-t-C_6-Pyr-Cer at 1-48 hr was detected by LC/MS in UM-SCC-22A cells after differential centrifugation, as described in Materials and Methods. C) The purity of mitochondria- and nuclei-enriched fractions (lanes 1 and 2, respectively) isolated from the UM-SCC-22A cells was analyzed by detecting the levels of cytochrome C (lower panel) and lamin B (upper panel) proteins using Western blotting as described in Materials and Methods. D) The growth inhibitory effects of L-t-C_6-Pyr-Cer against UM-SCC-22A, UM-SCC-14A and UM-SCC-1 cells were assessed by MTT assays after treatment of cells with increasing concentrations of the compound for 48 hr. Experiments were done in duplicates at least in three independent trials, and error bars represent standard deviations. When not seen, error bars are smaller than the diameter of the legends on the graphs. Statistical significance was determined using student's t-test, and $p<0.05$ (*) was considered significant.

Fig. 2. Synergistic effects of L-t-C_6-Pyr-Cer, in combination with GMZ, on the growth and cell cycle profiles of UM-SCC-22A cells. A) The synergistic interactions of L-t-C_6-Pyr-Cer and GMZ in the inhibition of growth were examined by quantitative isobologram studies, as described in Materials and Methods. The IC_{50} concentrations of GMZ in the presence of increasing concentrations of L-t-C_6-Pyr-Cer were determined by MTT assays, and the data were plotted in isobolograms. A straight line joining points on x- and y-axes represent the

IC_{50} concentrations of GMZ and L-t-C_6-Pyr-Cer alone. The points on the isobologram representing the IC_{50} values of GMZ obtained in the presence of 100, 250 and 500 nM L-t-C_6-Pyr-Cer fell within the left of the straight line, which indicates synergism. The experiments were performed as triplicates in at least three independent experiments. Error bars represent standard deviations. B) The effects of L-t-C_6-Pyr-Cer (500 nM) and GMZ (50 nM), alone or in combination, on cell cycle profiles of UM-SCC-22A cells were determined by flow-cytometry, after 48 hr treatment, as described in Materials and Methods.

Fig. 3. The determination of pharmacokinetic parameters such as clearance from the serum, and bioaccumulation in various organs of L-t-C_6-Pyr-Cer *in vivo*. A and B) The levels of L-t-C_6-Pyr-Cer in the serum (A) or in the vital organs (B) of the BALB/c mice were measured by LC/MS after IP injection of the compound for various time points. The experiments were performed in two independent trials as duplicates, and error bars represent standard deviations. Statistical significance was determined using student's t-test, and $p<0.05$ (*) was considered significant.

Fig. 4. The role of L-t-C_6-Pyr-Cer as compared to its conventional analogue L-t-C_6-Cer in the inhibition of HNSCC tumor growth in vivo. The effects of L-t-C_6-Pyr-Cer and its conventional analogue L-t-C_6-Cer as single agents were determined in SCID mice harboring the UM-SCC-22A xenografts implanted in both flanks, as described in Materials and Methods. (A) The tumors were confirmed to be squamous cell carcinomas by histopathologic analysis after H&E staining. (B) The animals were treated with ceramides at 40 mg/kg/each every 4 days for 24 days (6 cycles), and untreated mice were used as

controls. In these experiments, each group contained 3 mice, harboring 6 tumors. Statistical analysis was performed as described in Materials and Methods, and $p<0.05$ (*) was considered significant.

Fig. 5. The therapeutic efficacy of L-t-C_6-Pyr-Cer and GMZ combination in the inhibition of HNSCC tumor growth and/or progression *in vivo*. A) *In vivo* therapeutic efficacy of L-t-C_6-Pyr-Cer in combination with GMZ was determined in SCID mice harboring the UM-SCC-22A xenografts implanted in both flanks, as described in Materials and Methods. The animals were treated with L-t-C_6-Pyr-Cer and GMZ at 40 mg/kg/each every 4 days for 20 days. The therapeutic effects of the 5-FU/CP combination in this HNSCC model were also examined. In these experiments, each group contained 6 mice, harboring 12 tumors, in this study. Error bars represent standard deviations, and p values were calculated as described in Materials and Methods. B) The accumulation of L-t-C_6-Pyr-Cer in tumor sites, or in the intestines and liver was measured by LC/MS after the completion of the study. The effects of GMZ on the levels of L-t-C_6-Pyr-Cer in these tissues were also examined by LC/MS, as described. Lipid measurements were done in animals (6 animals with 12 tumors/group), and error bars represent standard deviations. Statistical significance was determined using student's t-test, and $p<0.05$ (*) was considered significant.

Fig. 6. The effects of L-t-C_6-Pyr-Cer, alone or in combination with GMZ, on the levels of endogenous ceramides and SM in HNSCC tumors, *in vivo*. The effects of L-t-C_6-Pyr-Cer, alone or in combination with GMZ, on the levels of endogenous ceramides (A and B) in HNSCC tumors extracted from SCID mice (summarized in Fig. 5A and B) were examined

by LC/MS. The levels of C14-, C16-, C18-, C24-, C24:1-, dihydro-C16-ceramides, and sphingosine are shown in (A), and C18:1-, C20-ceramides, and dihydro-sphingosine, and sphingosine-1-phosphate levels are shown in (B). Lipid measurements in HNSCC tumors were performed in these animals by LC/MS (n=12/group), and error bars represent standard deviations. There were no significant changes in these levels.

Fig. 7. The role of L-t-C_6-Pyr-Cer, alone or in combination with GMZ, in the inhibition of telomerase in HNSCC tumors *in vivo*. The role of L-t-C_6-Pyr-Cer, alone or in combination with GMZ, in the regulation of telomerase activity (A), telomere length analysis (B), the levels of hTERT mRNA (C), and protein (D) in HNSCC tumors extracted from SCID mice after studies summarized in Fig. 5, were examined by TRAP, TRF, Q-PCR, and Western blotting, respectively, as described in Materials and Methods. In (B), DNA samples obtained from tumors treated with GMZ (G), L-t-C_6-Pyr-Cer (Cer), and the combination of L-t-C_6-Pyr-Cer with GMZ (G/C, lanes 3-5, respectively) were compared to that of untreated (U) tumors (lane 2). Lanes 5 and 6 contain DNA samples with low (L) and high (H) molecular weight (3.9 and 10.2 kb, respectively) telomeres. In (D) The levels of hTERT protein in samples obtained from tumors treated with GMZ (G), L-t-C_6-Pyr-Cer (Cer), and the combination of L-t-C_6-Pyr-Cer with GMZ (G/Cer, lanes 2-4, respectively) were determined by Western blot analysis using rabbit polyclonal anti-hTERT antibody, and compared to that of untreated (U) tumors (lane 1). Lanes 5 and 6 contain samples from telomerase positive (+) and negative (-) extracts. Beta-actin levels of these samples were used as loading controls (lanes 1-6, lower panel). Statistical significance was determined using student's t-test, and $p<0.05$ (*) was considered significant.

Tables

TABLE 1

Determination of the MTD of L-t-C_6-Pyr-Cer *in vivo.*

MTD of L-t-C_6-Pyr-Cer was determined in dose escalation studies, in which BALB/c mice were treated (by IP injections) with increasing concentrations of the compound (10-150 mg/kg), dissolved in sterile saline solution, for 24 hr. The MTD of the compound was assessed as 80 mg/kg, which did not result any detectable toxicity in any of the animals. The toxic concentrations of the compound at or >100 mg/kg caused severe abdominal bloating, and intestinal malfunction. Possible toxicity of the compound to the vital organs of the animals was analyzed by both gross examination, and histopathology.

Group	Dose (mg/kg)	Total animals	Percent Mortality	Toxicity
1	10	4	0	none
2	20	4	0	none
3	40	4	0	none
4	60	4	0	none
5	80	10	0	none
6	100	10	10	N.D.
7	120	10	20	abdominal bloating
8	150	4	50	abdominal bloating, intestinal malfunction

N.D., not determined

JPET Fast Forward. Published on March 1, 2006 as DOI: 10.1124/jpet.106.101949
This article has not been copyedited and formatted. The final version may differ from this version.

TABLE 2

Determination of the effects of L-t-C_6-Pyr-Cer on the blood counts, the levels of enzymes and electrolytes in serum *in vivo*.

The blood counts, the levels of serum enzymes, and electrolytes in response to L-t-C_6-Pyr-Cer (Pyr-Cer) alone or in combination with GMZ in SCID mice by Anilytics, Inc. (Gaithersburg, MD), as described in Materials and Methods. Pyridinium ceramide did not have any detectable effects on these parameters, which were within the normal levels (ranges) in these animals. The data shown here represent the blood work of one of the animals from each group.

Treatment	RBC	Hemoglobin	BUN	Creatinine	Na	Mg	ALT	Amylase
Control	8.0	13.9	19	0.4	145	3.1	24	763
Pyr-Cer	8.4	14.1	23	0.6	142	2.7	52	1589
GMZ/Cer	n.d.	n.d.	36	0.5	147	3.1	23	1526

RBC, red blood cells; BUN, blood urea nitrogen; ALT, Alanine aminotransferase.

The units: RBC (1 x 10^6 cells/µl), hemoglobin (gm/100 ml), BUN and creatinine (mg/100 ml), GGTand amylase (unit/l), electrolytes (mmole/l).

Figure 1

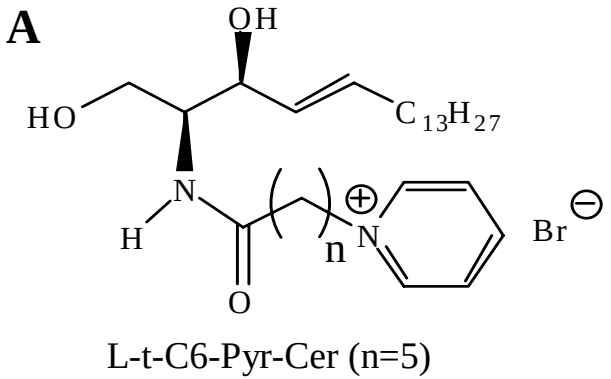

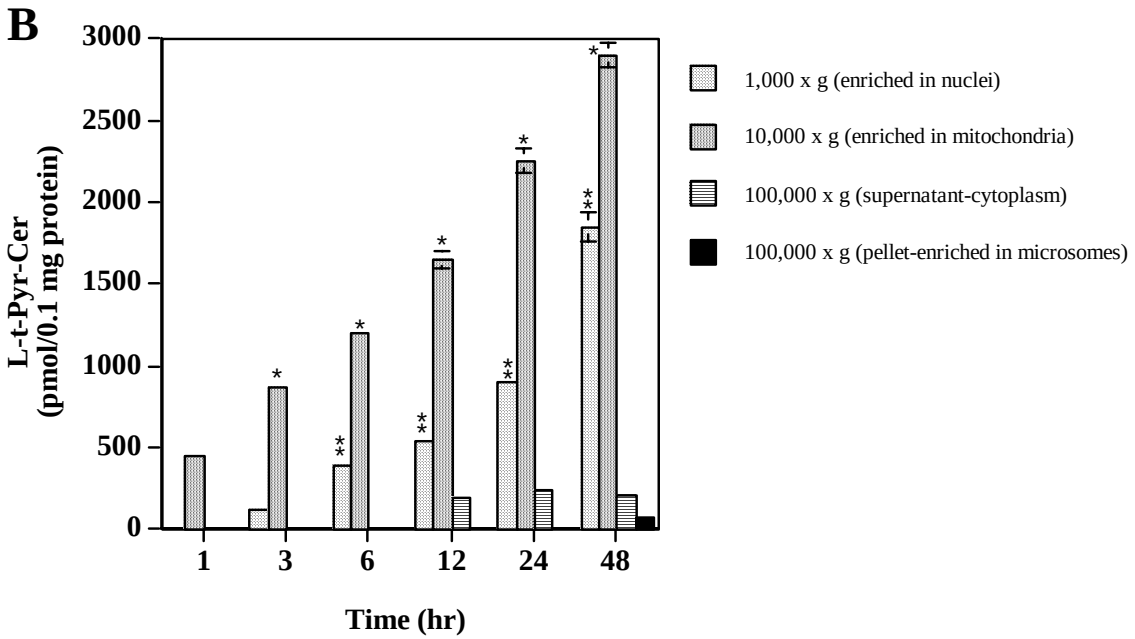

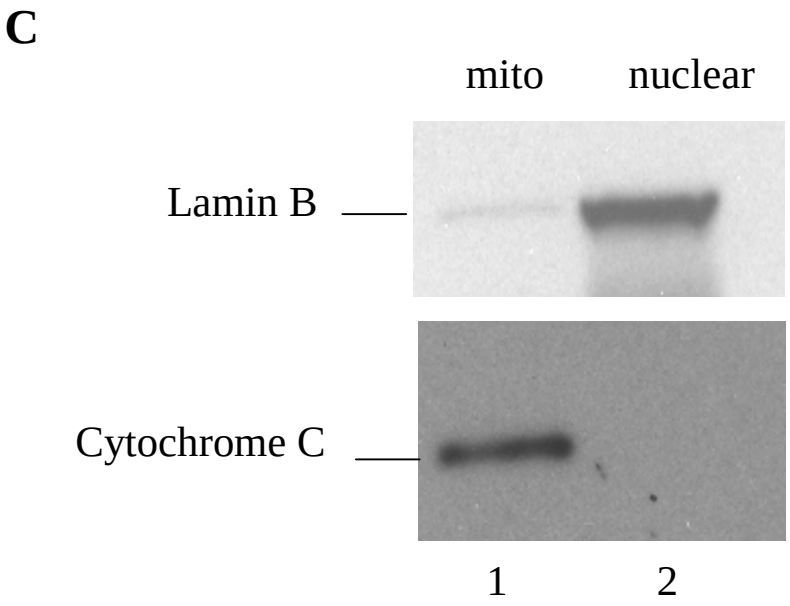

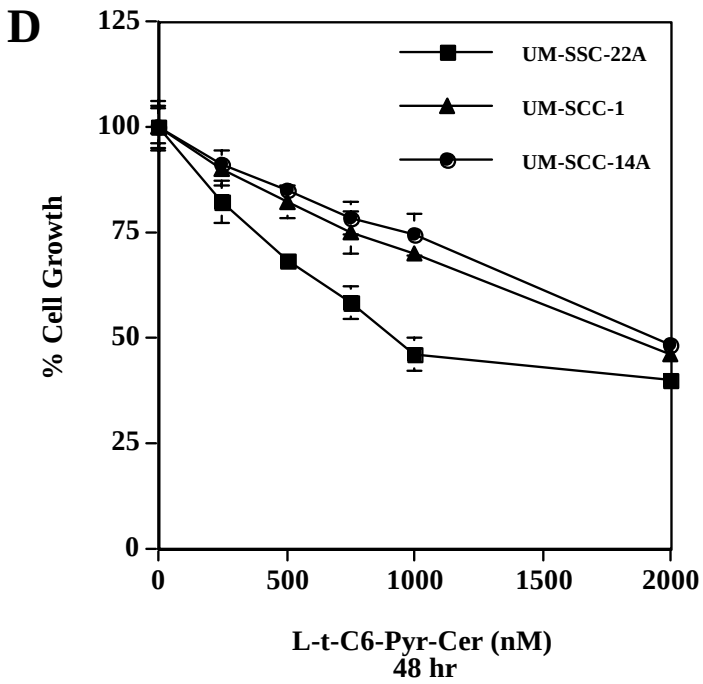

Figure 2

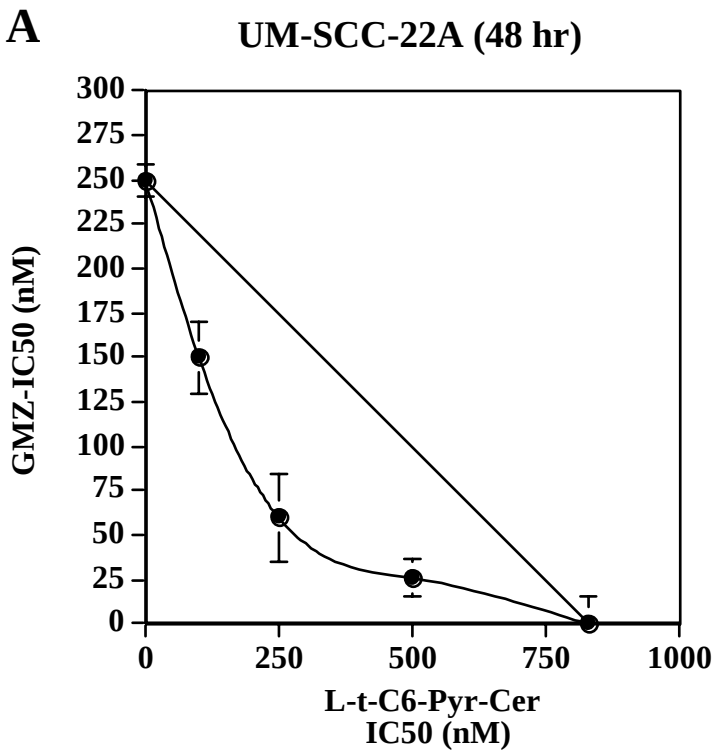

B

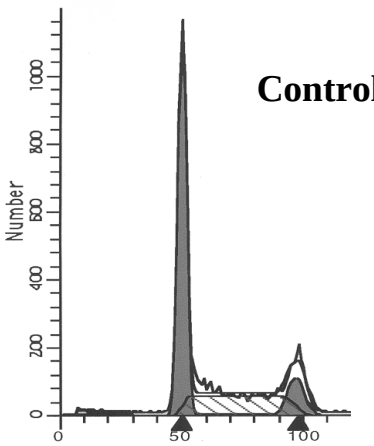

Cell Cycle	% Cell Population
G0/G1	55.4
S	33.2
G2M	11.4
Apoptosis	1.3

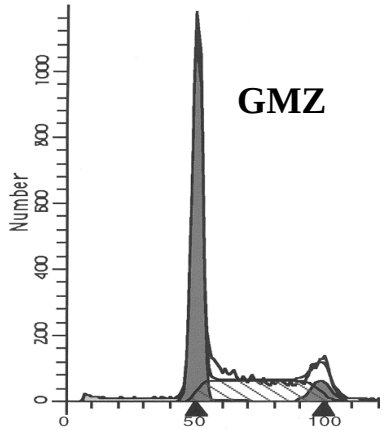

Cell Cycle	% Cell Population
G0/G1	58.7
S	34.5
G2M	6.8
Apoptosis	0.07

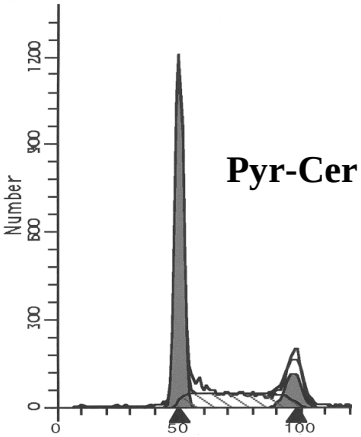

Cell Cycle	% Cell Population
G0/G1	59.9
S	28.1
G2M	12.0
Apoptosis	0.00

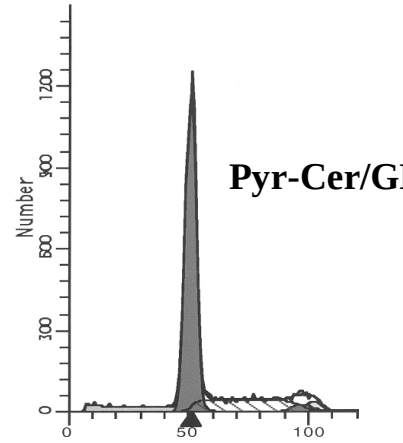

Cell Cycle	% Cell Population
G0/G1	74.2
S	22.5
G2M	3.3
Apoptosis	0.1

Figure 3

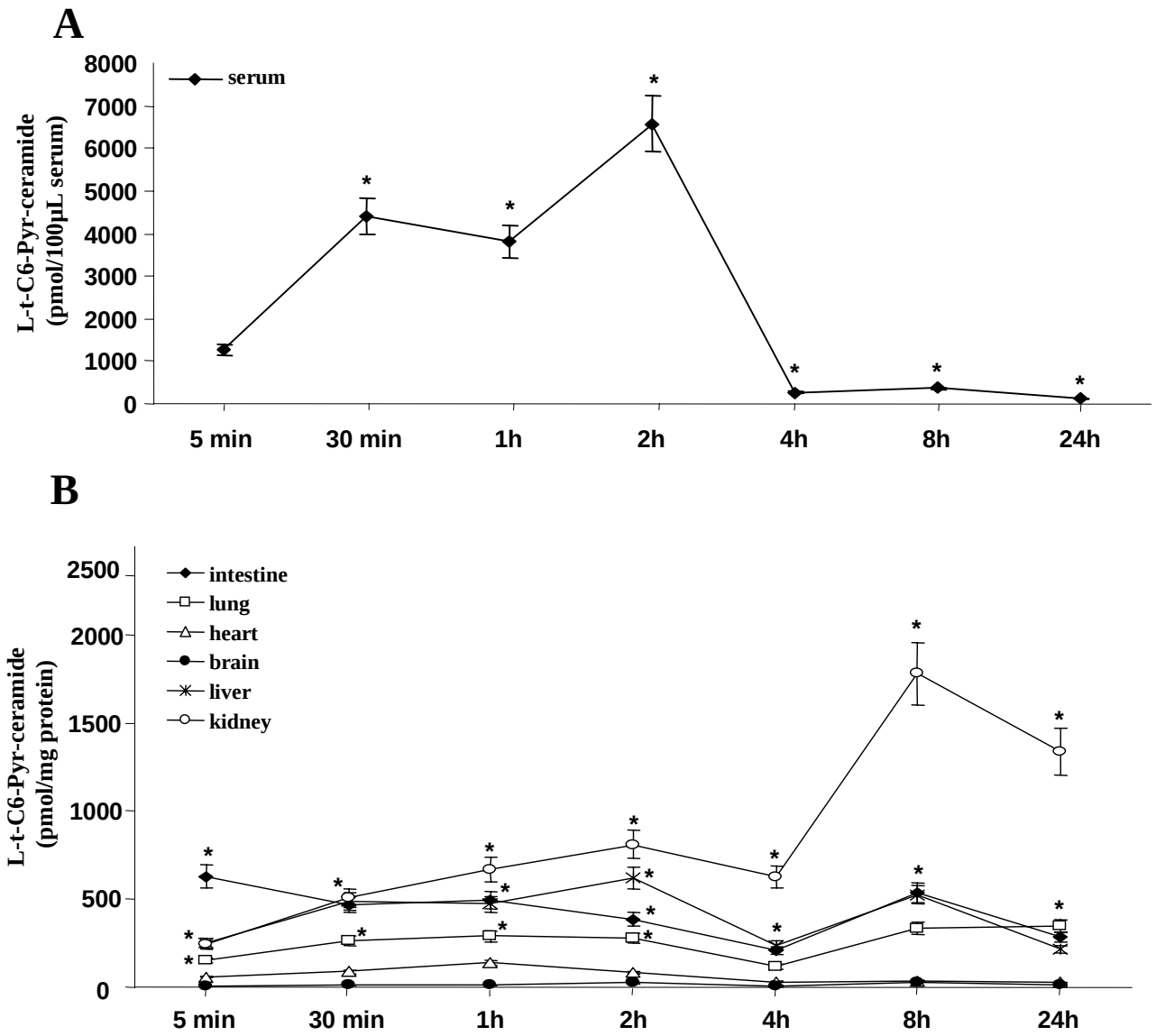

Figure 4

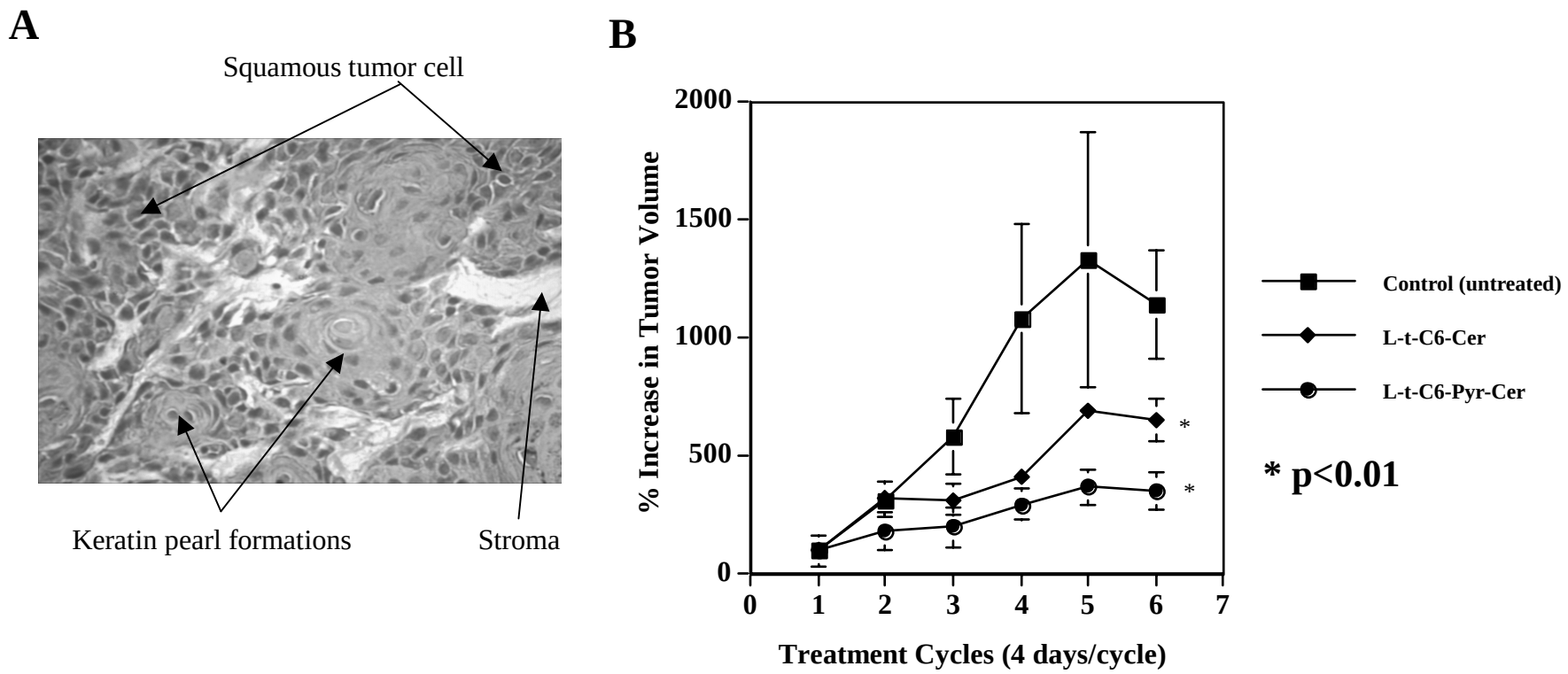

Figure 5

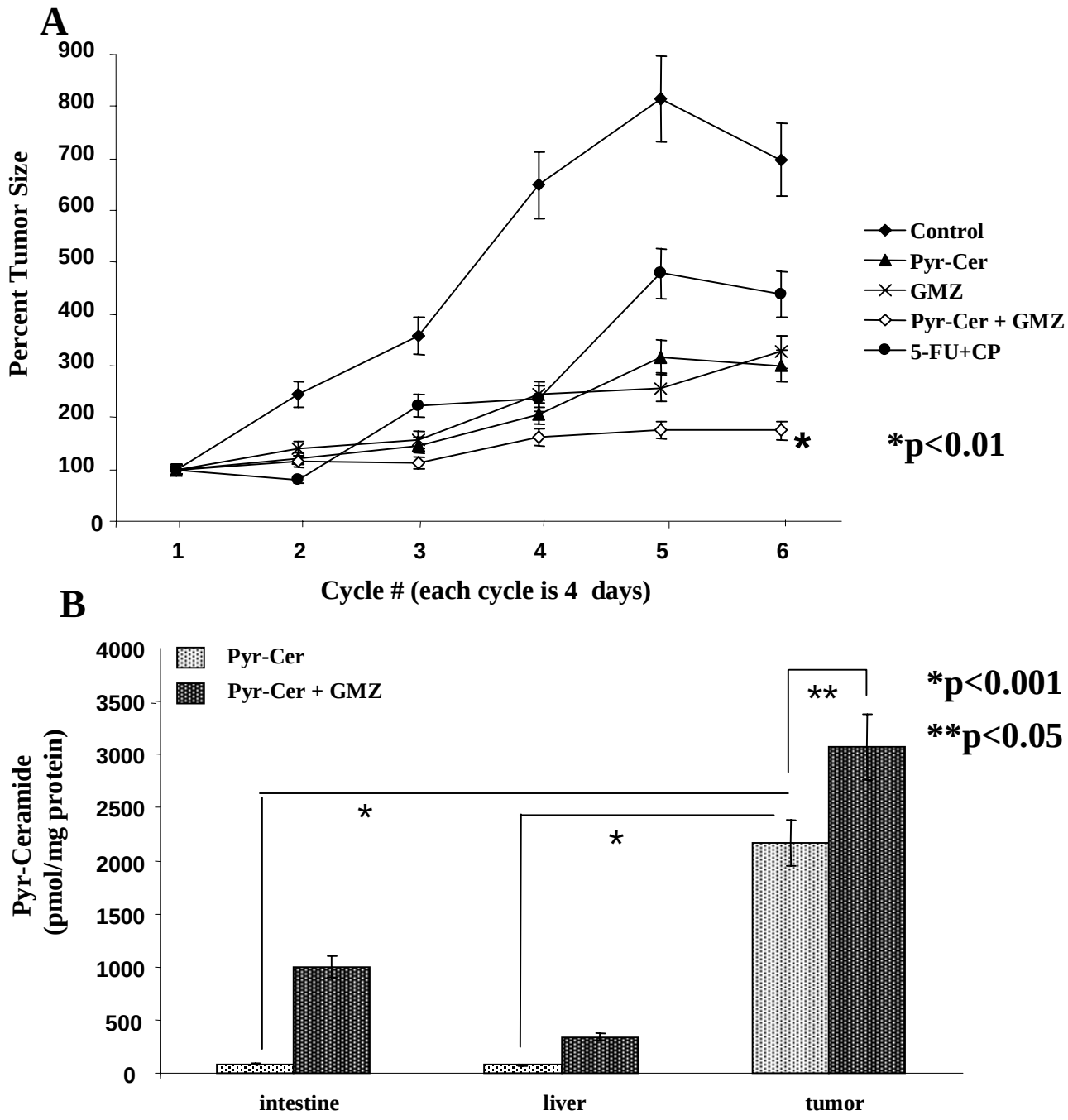

Figure 6

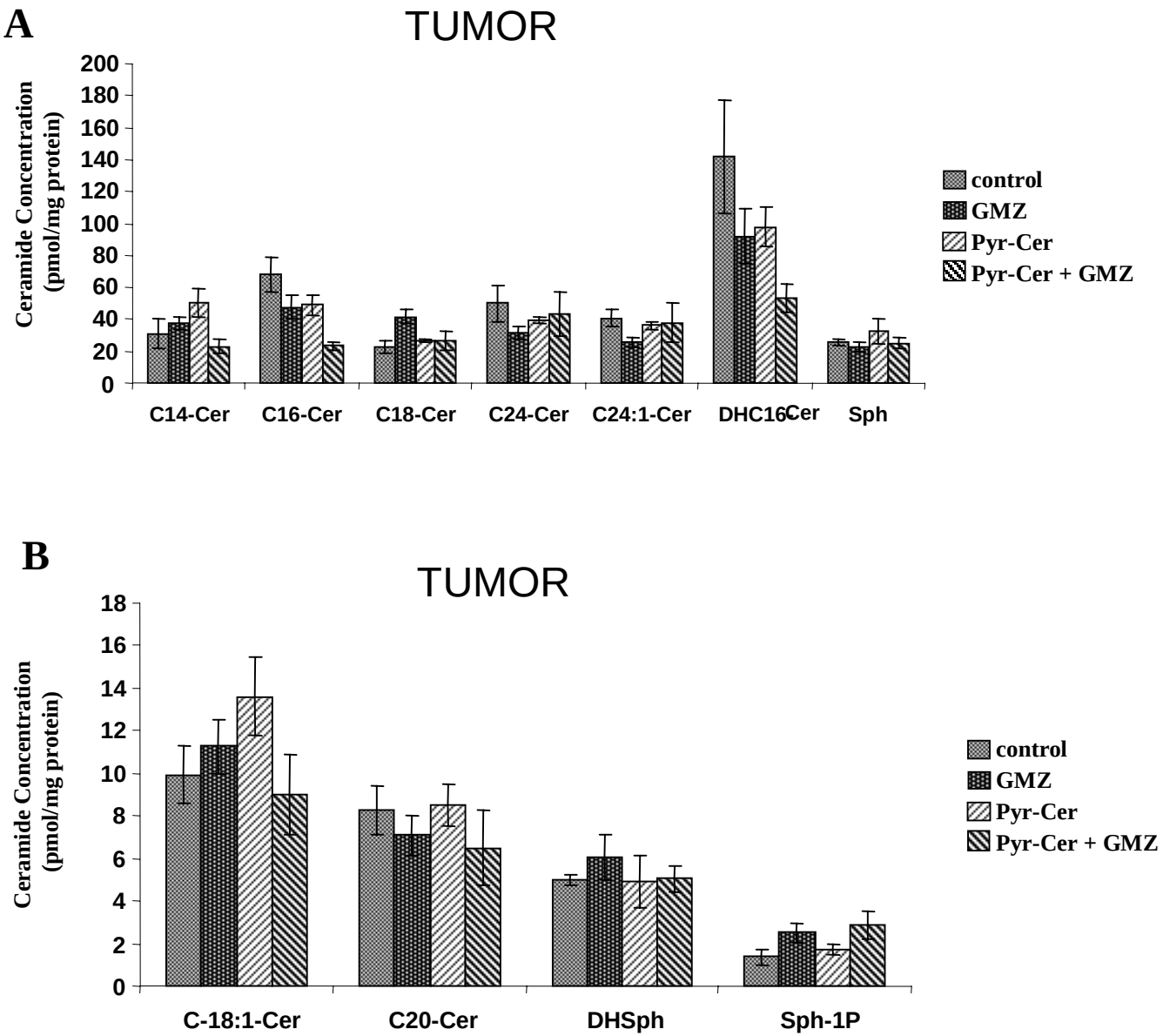

Figure 7